Electronic supplementary information

Tuning the surface structure of Fe-based catalyst for transfer hydrogenation of nitroarenes at near room temperature

Dan Wu[a], Shuchang Wu[a,b,c*], Jinliang Liu[d], Xiaomin Zhang[d], Xiaomin Fang[d], Shuchun Li[d], Yiquan Chen[d*], Zailai Xie[c,d*]

[a] *School of Materials and Chemical Engineering, Ningbo University of Technology, 201 Fenghua Road, Ningbo 315211, China*
[b] *Zhejiang Institute of Tianjin University, Ningbo 315201, China*
[c] *State Key Laboratory of Photocatalysis on Energy and Environment, Fuzhou University, Fuzhou 350016, China*
[d] *Key Laboratory of Advanced Carbon-Based Functional Materials (Fujian Province University), Fuzhou University, Fuzhou 350016, China*

*Corresponding author.
E-mail address: scwu10b@alum.imr.ac.cn (S. Wu); T08028@fzu.edu.cn (Y. Chen); zlxie@fzu.edu.cn (Z. Xie)

Experimental

Materials

Guanine (99%), 2-methylimidazole (98%), 4-nitrofluorobenzene (98%), 4-nitrochlorobenzene (99.5%), 1-bromo-4-nitrobenzene (99%), 4-nitroiodobenzene (98%), 4-nitrotoluene (99%), 4-ethylnitrobenzene (99%), 2-nitrophenol (99%), 3-nitrophenol (99%), 4-nitrophenol (99%), 2-nitrobenzyl alcohol (98%), 4-nitroaniline (99%), 1,3-dinitrobenzene (99%), 4-nitroanisole (98%), 8-nitroquinoline (98%), 2-nitrofluorene (98%), 5-nitroindole (98%) and 2-chloro-3-nitropyridine (99%) were supplied by Aladdin Reagent Co. Ltd., Shanghai, China. Nitrobenzene (99%), hydrazine hydrate (85%), ferric nitrate nonahydrate (99%), formic acid (99%), sodium borohydride (AR), L-ascorbic acid (99%), isopropanol (99%) and sodium sulfide nonahydrate (98%) were purchased from China Medicine Group Shanghai Chemical Reagent Company. All the reagents were used without further purification.

Synthesis of the catalyst

The catalyst was synthesized through the carbonization of guanine and iron precursor under noble gas atmosphere. Typically, 1.314 g of 2-methylimidazole was dissolved in 50 mL of water to form solution A. Next, 0.808 g of ferric nitrate nonahydrate ($Fe(NO_3)_3 \cdot 9H_2O$) was placed in another beaker and added 50 mL of water to obtain solution B. Then, solution B was added to solution A with the assistance of a pipette and kept stirring for 6 h at room temperature. Afterwards, 5 g of guanine was dispersed in 50 mL of water and added to the above mixture that made of 2-methylimidazole and $Fe(NO_3)_3 \cdot 9H_2O$. Two hours later, the catalyst precursor was obtained by centrifugation and washing with water. After drying in a 65 °C oven, the catalyst precursor was placed in a quartz boat, which subsequently transferred to a quartz tube that placed in a tube furnace. Then, the temperature of the furnace elevated to 800 °C with a heating rate of 5 °C/min. After carbonization for 1 h in the protection of N_2, the catalyst was taken out after the furnace cooled down to room temperature. The obtained sample was denoted as FeNC800. Similarly, FeNC700 and FeNC900 was prepared under the sample procedure, except that the carbonization temperature was

700 and 900 °C, respectively. FeNC800-woM was fabricated without the addition of 2-methylimidazole, while B-FeNC800 was synthesized in the absence of guanine. NC800 was harvested by direct carbonization of guanine at 800 °C in N_2 flow.

Characterization

The X-ray diffraction (XRD) patterns were collected on a Rigaku D/Max-2500PC diffractometer with a Cu Kα radiation source operating at 50 kV, 300 mA. The Raman spectra were recorded using a Renishaw inVia with a 532 nm laser excitation. The nitrogen adsorption-desorption isotherms were acquired from Micromeritics ASAP 2020 HD88 at 77 K. The specific surface area was calculated by Brunauer-Emmett-Teller (BET) method, while the pore size distributions were evaluated from the desorption branches of the isotherms using the Barrett-Joyner-Halenda (BJH) method. The X-ray photoelectron spectroscopy (XPS) spectra were collected on an ESCALAB 250 XPS system with a monochromatized Al Kα X-ray source (1486.6 eV) with correction for cross sections and escape depths. The transmission electron microscopy (TEM), high angle annular dark field scanning TEM (HAADF-STEM) and *in-situ* TEM were carried out on a FEI Talos F200S G2 microscope (operated at 200 kV) combined with an energy dispersive spectroscopy (EDS) spectrometer.

Catalytic evaluation of the materials

The reduction of nitroarenes was performed at near room temperature over the as-synthesized catalyst. In specific, 10 mg of FeNC800 catalyst was added to a 15 mL glass reactor, followed by the addition of 1 mmol of nitrobenzene and 4 mmol of hydrazine monohydrate. Then, the glass reactor was sealed with a teflon lid and immersed in a 30 °C water bath and kept for certain time. After the reaction, the mixture was analyzed by GC. The reduction of substituted nitroaromatic was carried out under similar condition.

**Text S1: Additional description of the XRD results in Fig. 1a in main article**

As for FeNC900, the diffraction peaks for Fe_3C disappeared, but notable peaks centered at 44.7, 65.0 and 82.3° appeared, which could be originated from the (110), (200) and (211) plane of metallic Fe, respectively (JCPDS PDF#87-0721). Meanwhile, the peak at 35.4° could be indexed to (311) plane of Fe_3O_4 (JCPDS PDF#79-0416).

Text S2: Additional description of high resolution Fe2p analysis results in Fig. 1f in main article

The peaks at 710.7 and 713.2 eV were ascribed to Fe^{2+} $Fe2p_{3/2}$ and Fe^{3+} $Fe2p_{3/2}$, while that located at 724.0 and 726.7 eV were attributed to Fe^{2+} $Fe2p_{1/2}$ and Fe^{3+} $Fe2p_{1/2}$. Meanwhile, the peaks centered at 716.5 and 720.3 eV were assigned to the satellite peaks for Fe^{2+} and Fe^{3+}, respectively. Besides, a peak at 707.4 eV derived from Fe-C could be observed, indicating the presence of iron carbide.
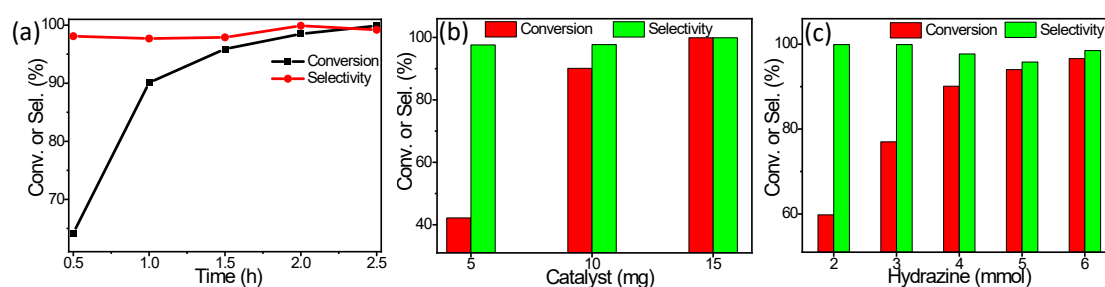
Fig. S1. The effect of reaction time (a), catalyst loading (b) and hydrazine dosage (c) on the reduction of nitrobenzene
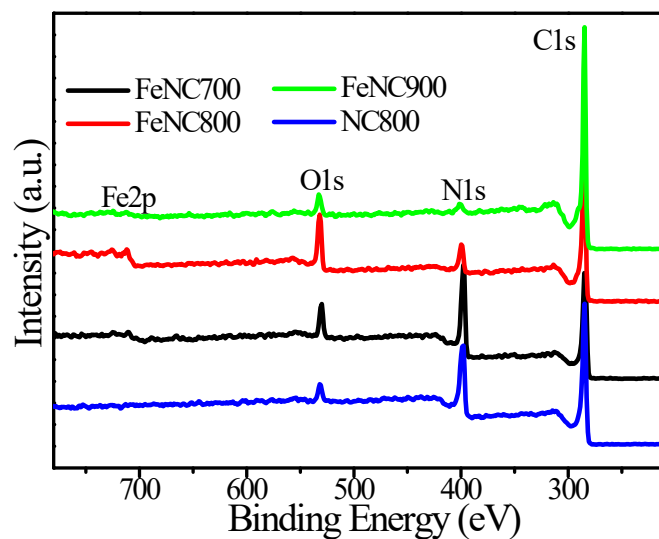
Fig. S2. XPS scan spectra of the samples
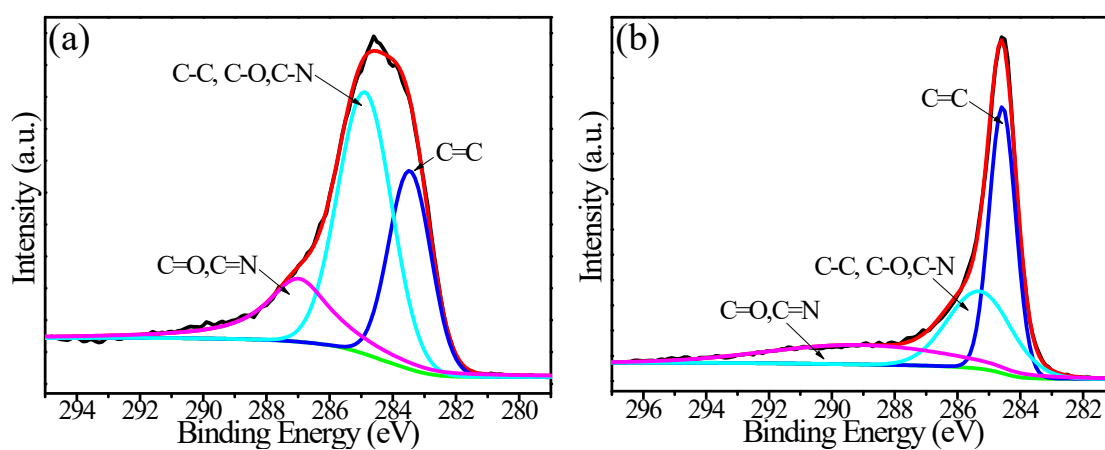
Fig. S3. High resolution C1s spectra of FeNC700 (a) and FeNC900 (b)
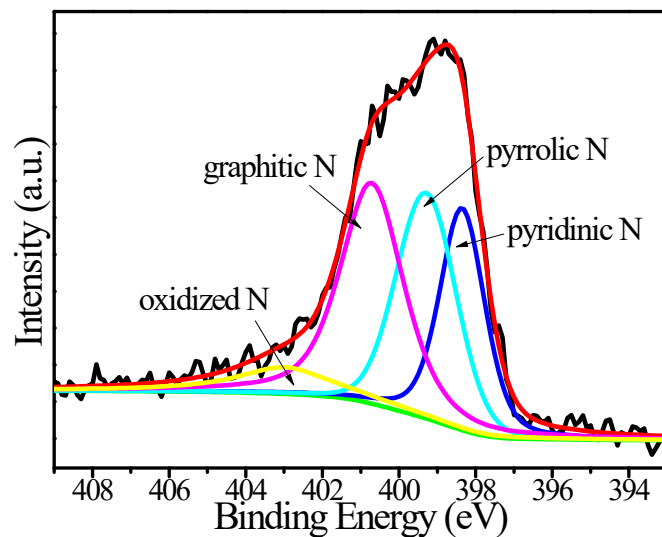
Fig. S4. High resolution N1s spectra of FeNC800
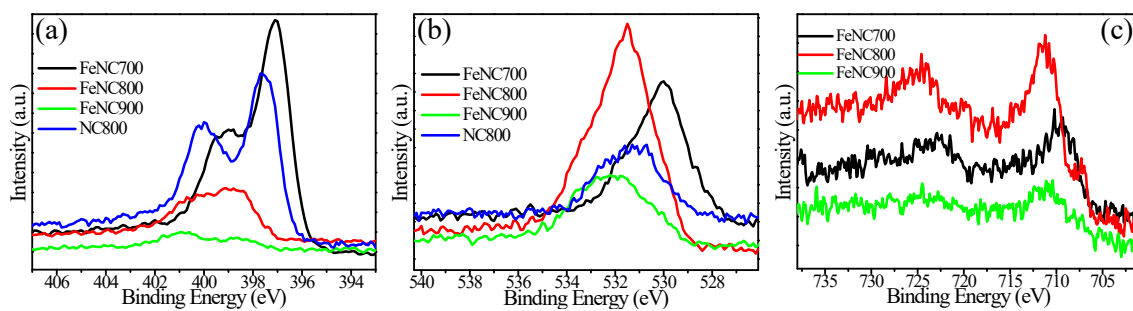
Fig. S5. N1s (a), O1s (b) and Fe2p spectra of the materials
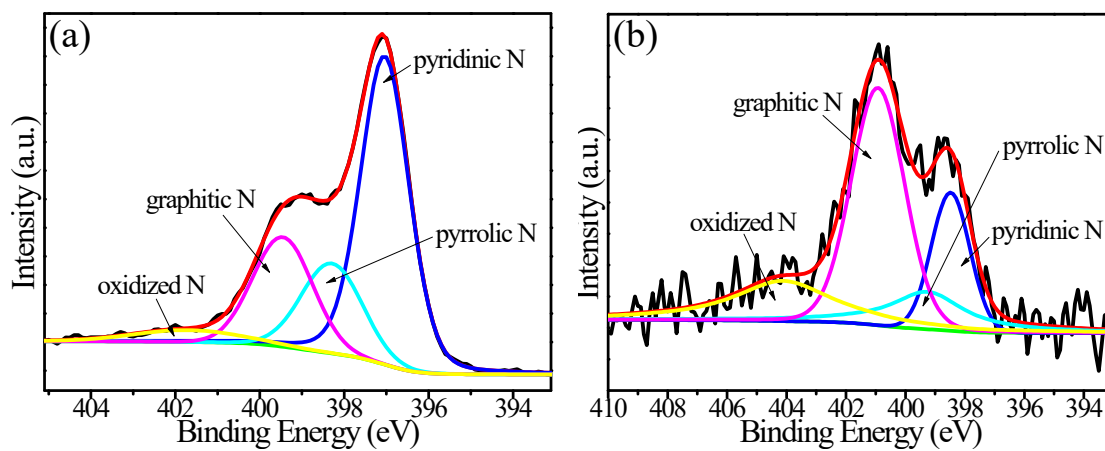
Fig. S6. High resolution N1s spectra of FeNC700 (a) and FeNC900 (b)
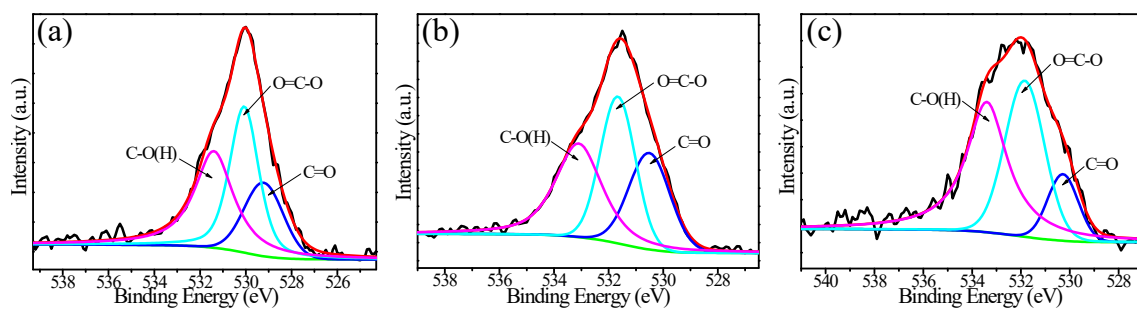
Fig. S7. High resolution O1s spectra of FeNC700 (a), FeNC800 (b) and FeNC900 (c)
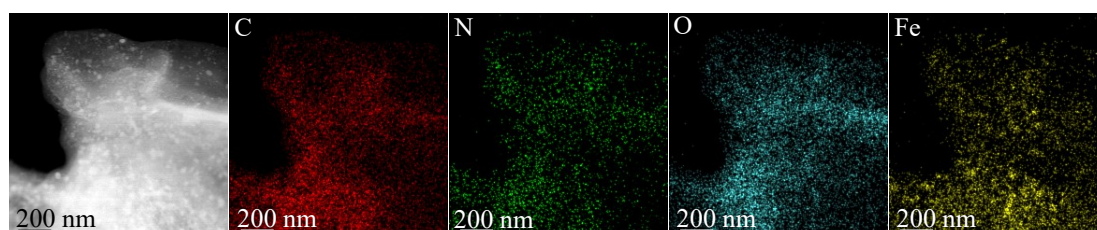
The high resolution O1s spectrum of materials indicated the presence of three kinds of O species. The peaks centered at 530.5, 531.7 and 533.1eV was ascribed to C=O, O=C-O and C-O(H), respectively [1,2].
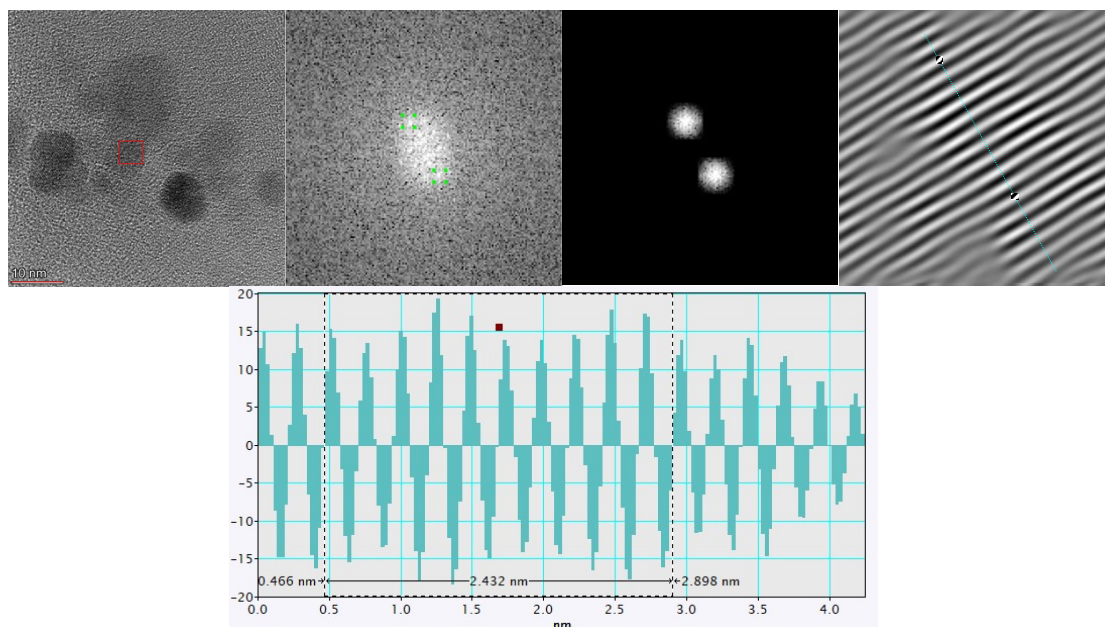
Fig. S8. HRTEM of FeNC700
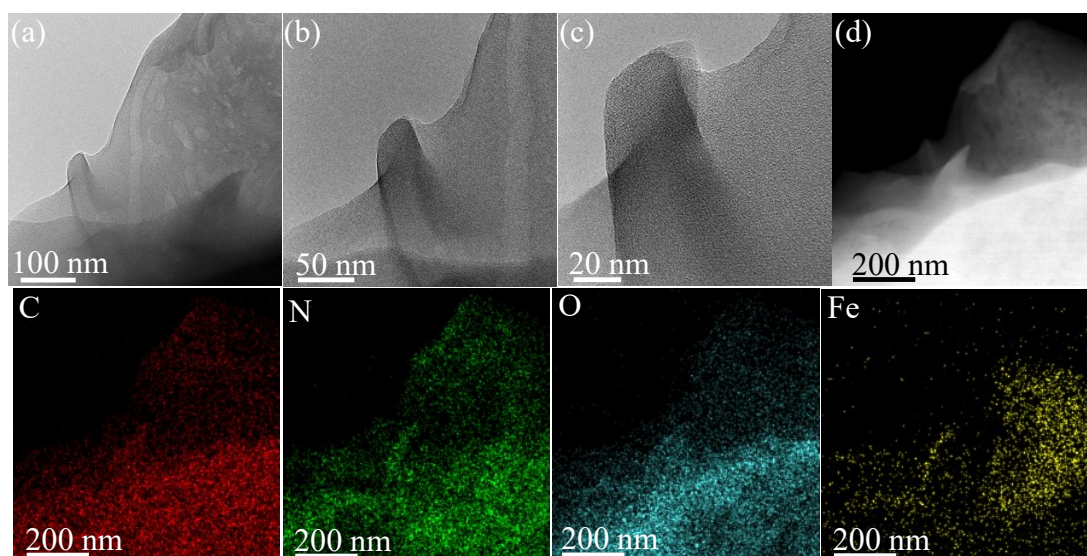
Fig. S9. TEM (a-c) and HAADF-STEM combined with EDX mapping images (d) of FeNC700

Fig. S10. HAADF-STEM combined with EDX mapping images of FeNC800
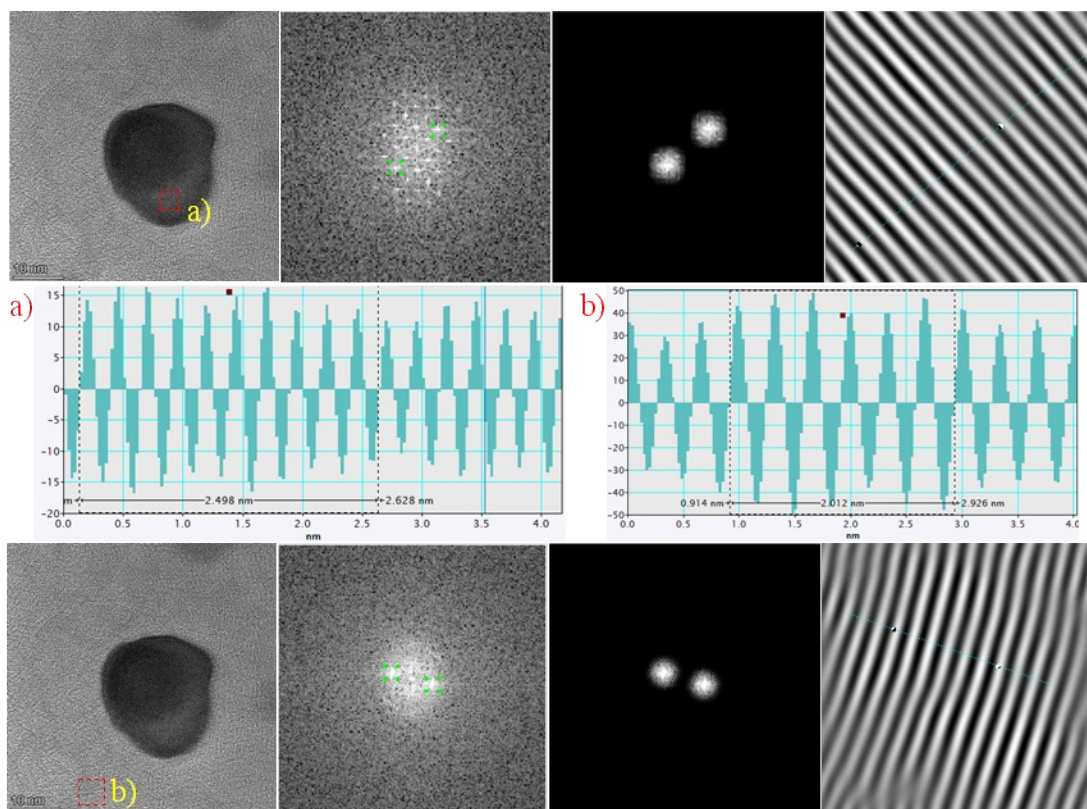
Fig. S11. HRTEM of FeNC800
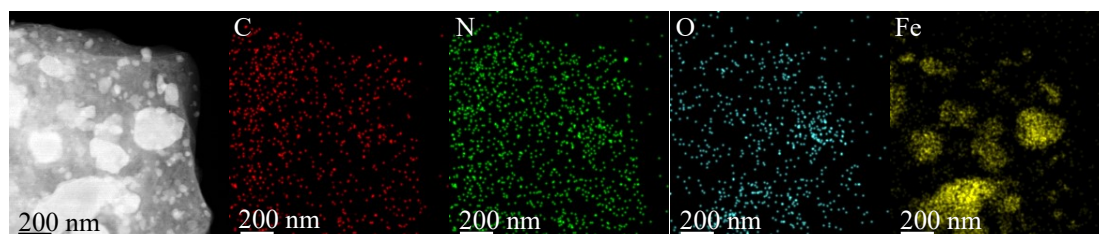
Fig. S12. HAADF-STEM combined with EDX mapping images of FeNC900
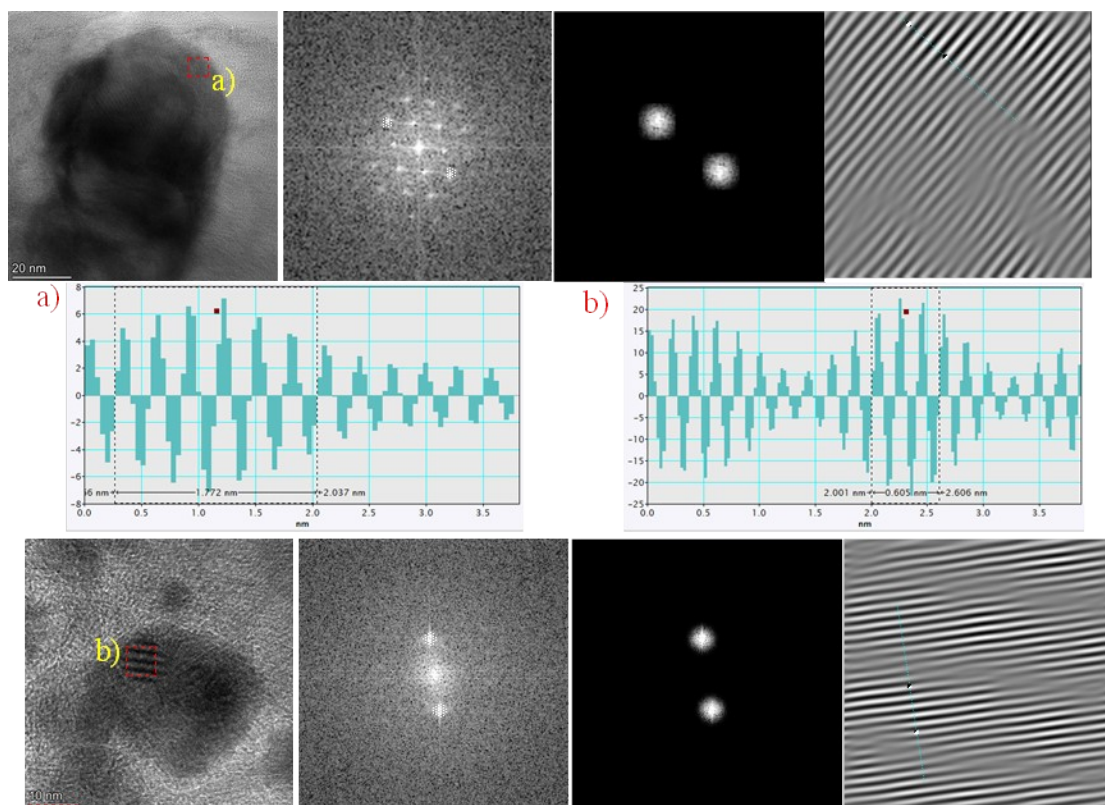
Fig. S13. HRTEM of FeNC900
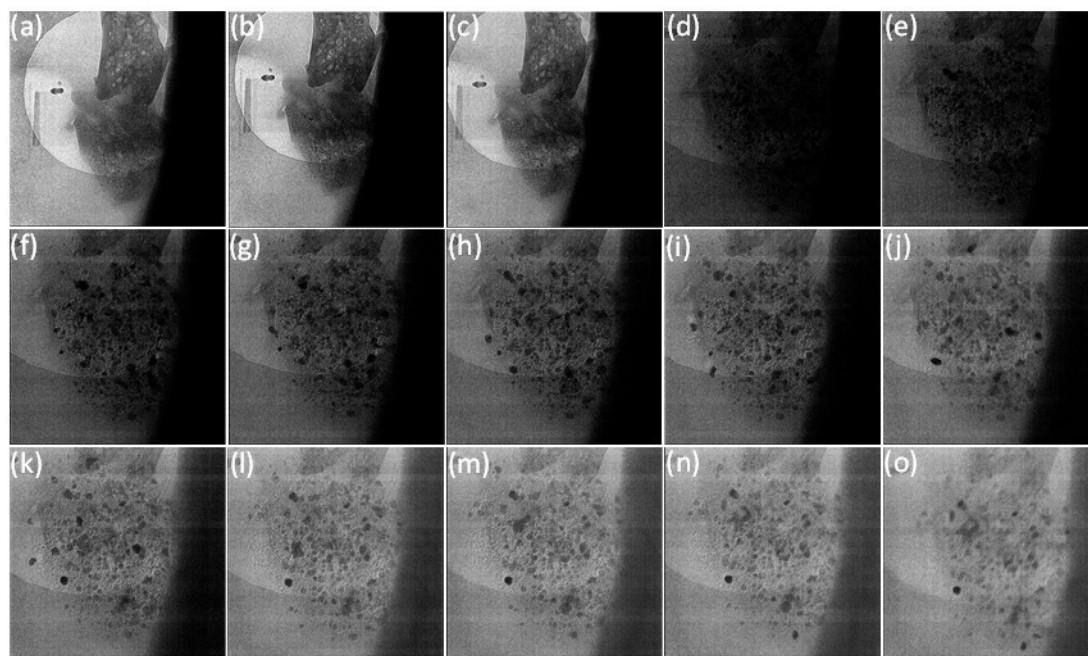
Fig. S14. The surface evolution of FeNC700 when heated to 800 °C
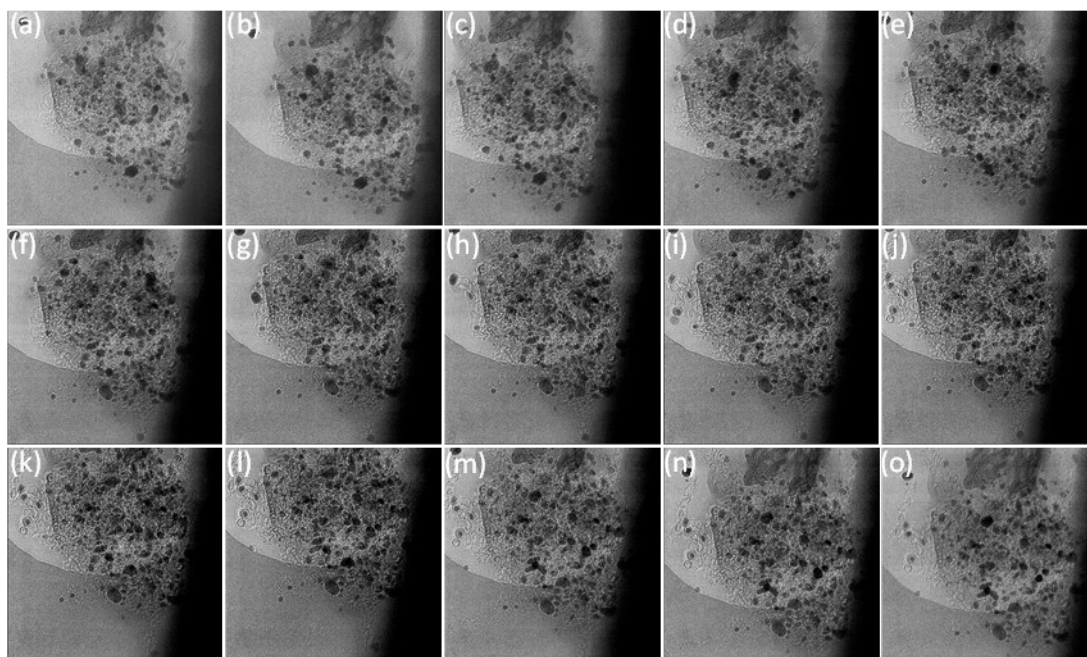
Fig. S15. The surface evolution of FeNC700 when heated from 800 °C to 900 °C
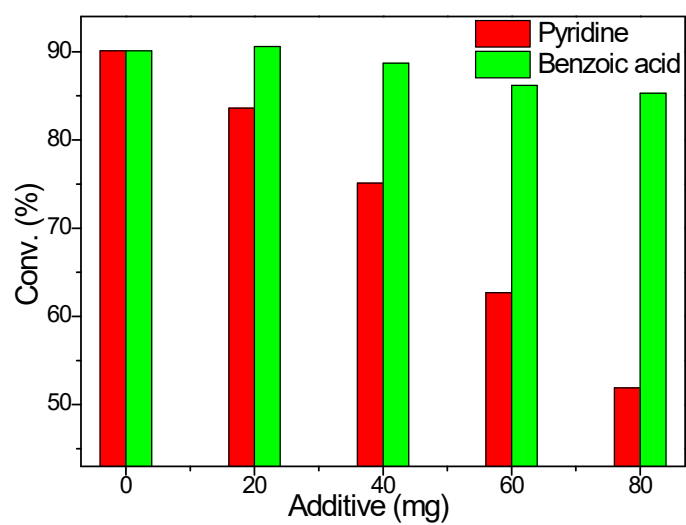
Fig. S16. The effect of pyridine and benzoic acid on the reaction

Condition: 10 mg of FeNC800, 4 mmol of hydrazine hydrate, a certain amount of

pyridine or benzoic acid, 30 °C, 1 h.
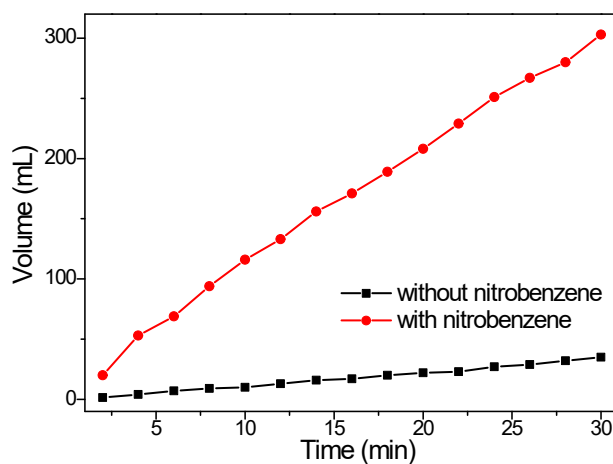
Fig. S17. Decomposition of hydrazine hydrate over FeNC800

Condition: 10 mg of FeNC800, 3.0 g of hydrazine hydrate, 1.5 g of nitrobenzene, 30°C.
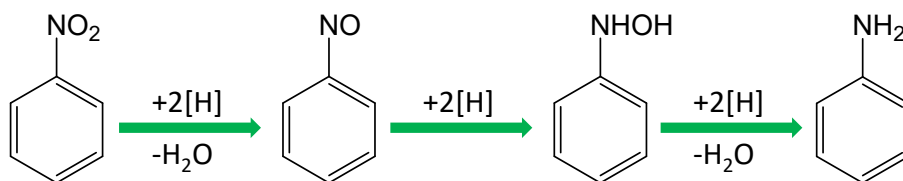
Fig. S18. Proposed reaction mechanism for nitrobenzene reduction

Nitrobenzene adsorbed on the carbon matrix through π-π interactions. On the other hand, hydrazine was adsorbed on Fe_3C and was activated. Then, $-NO_2$ groups abstracted two active [H] from hydrazine and converted to -NO groups. Next, -NO was reduced by two active [H] to -NHOH, which finally converted to $-NH_2$ through the reduction of two active [H]. After desorption of aniline, the active site was regenerated and took part in next catalytic circle.
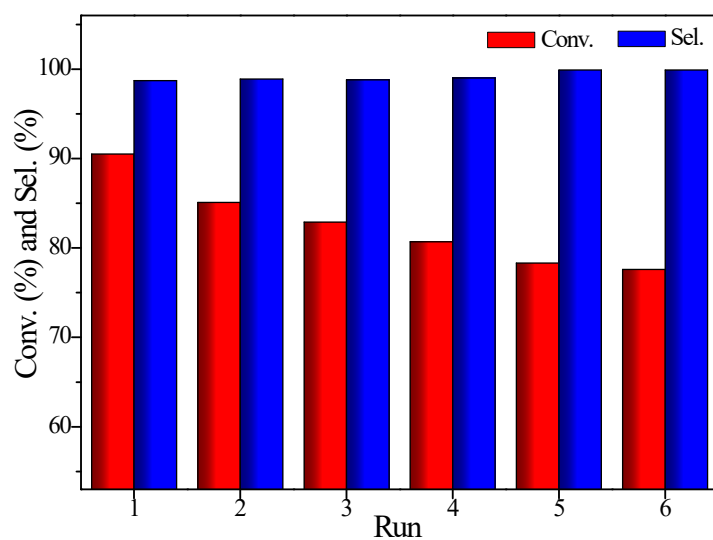
Fig. 19. The recyclability of FeNC800
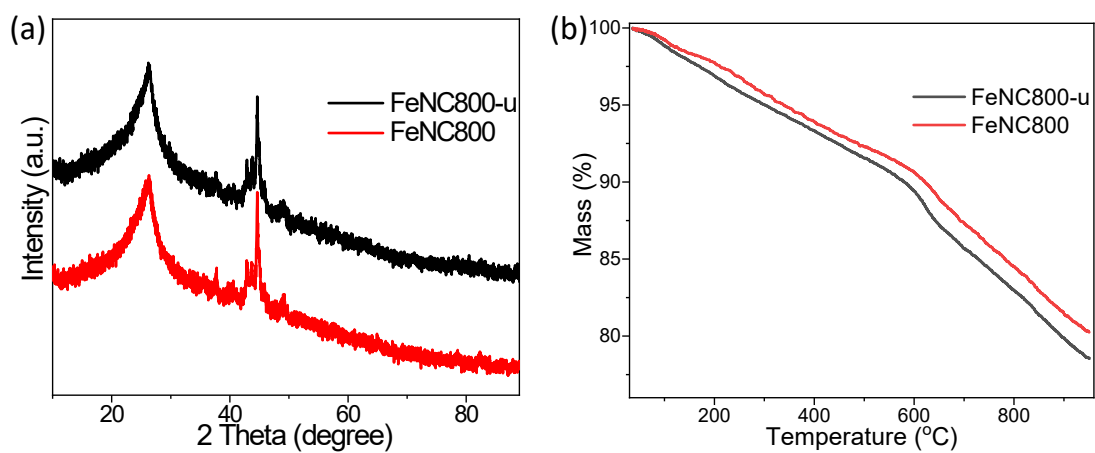
Fig. S20. XRD patterns (a) and TG curves (b) of the fresh and spent catalysts

Table S1. Surface area, pore volume and average diameter of the materials

Sample	S_{BET} (m^2/g)	S_{micro} (m^2/g)	V_{total} (cm^3/g)	V_{micro} (cm^3/g)	D (nm)
FeNC700	51.6	20.3	0.105	0.00950	9.6
FeNC800	142.0	39.0	0.249	0.0176	6.1
FeNC900	114.4	20.4	0.266	0.00936	6.7
NC800	93.0	29.0	0.223	0.0133	8.0

Table S2. Surface content of each element on different catalysts
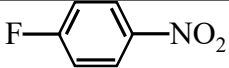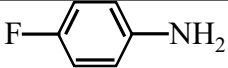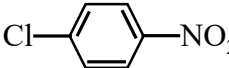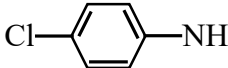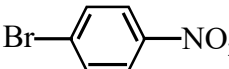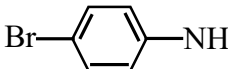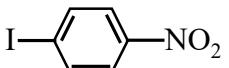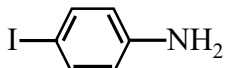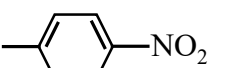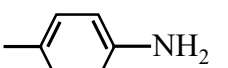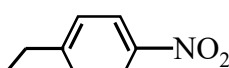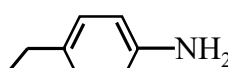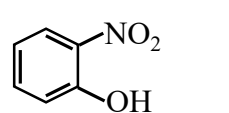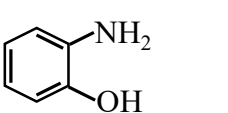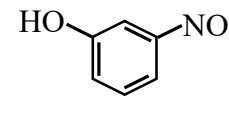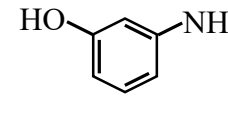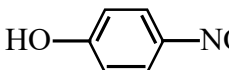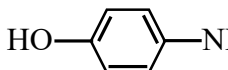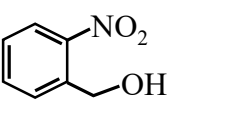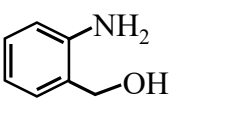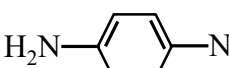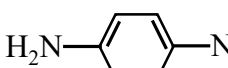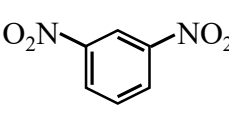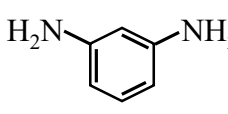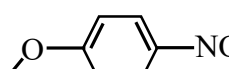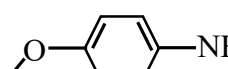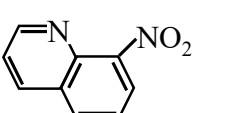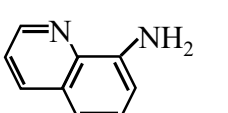
Catalyst	C (at%)	N (at%)	O (at%)	Fe (at%)
FeNC700	58.53	32.3	7.81	1.36
FeNC800	75.58	11.17	11.32	1.94
FeNC900	90.87	3.7	4.62	0.81
NC800	69.07	26.28	4.64	0
FeNC800-u	75.52	11.46	11.08	1.94
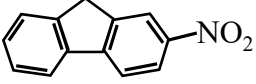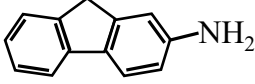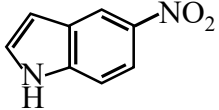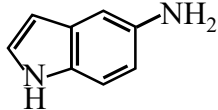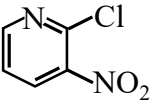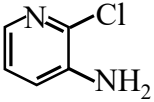
Table S3. Reduction of azobenzene to aniline over FeNC800

Entry	Time (h)	Conv. (%)	Sel. (%)
1	0.5	76.6	<1
2	1.0	92.9	<1

Condition: 10 mg of FeNC800, 0.3 mmol of azobenzene, 4 mmol of hydrazine hydrate, 30 ºC.

Table S4. Reduction of substituted nitroarenes

Entry	Substrate	Product	Conv. (%)	Sel. (%)
1 [a]	F—⬡—NO₂	F—⬡—NH₂	99.9	88.2
2 [a]	Cl—⬡—NO₂	Cl—⬡—NH₂	99.9	99.9
3 [b]	Br—⬡—NO₂	Br—⬡—NH₂	99.9	99.9
4 [b]	I—⬡—NO₂	I—⬡—NH₂	99.9	99.9
5 [c]	—⬡—NO₂	—⬡—NH₂	99.9	99.9
6 [c]	Et—⬡—NO₂	Et—⬡—NH₂	99.9	99.9
7 [c]	o-NO₂, OH	o-NH₂, OH	99.9	99.9
8 [c]	HO—⬡—NO₂	HO—⬡—NH₂	99.9	99.9
9 [c]	HO—⬡—NO₂	HO—⬡—NH₂	99.9	99.9
10 [c]	o-NO₂, CH₂OH	o-NH₂, CH₂OH	99.9	99.9
11 [d]	H₂N—⬡—NO₂	H₂N—⬡—NH₂	99.9	99.9
12 [d]	O₂N—⬡—NO₂	H₂N—⬡—NH₂	99.9	99.9
13 [d]	MeO—⬡—NO₂	MeO—⬡—NH₂	99.9	99.9
14 [e]	quinolin-8-yl-NO₂	quinolin-8-yl-NH₂	99.9	99.9

15 [e]	fluorene-2-NO$_2$ structure	fluorene-2-NH$_2$ structure	99.9	99.9
16 [e]	5-NO$_2$ indole structure	5-NH$_2$ indole structure	99.9	99.9
17 [e]	2-Cl-3-NO$_2$ pyridine structure	2-Cl-3-NH$_2$ pyridine structure	99.9	80.3

Reaction condition: 10mg FeNC800, 1mmol substrate, 4mmol hydrazine hydrate, 1 mL ethanol, 30°C. [a] 25°C, 0.5 h. [b] 0.5 h. [c] 1.5 h. [d] 3h. [e] 0.5mmol substrate, 1.5h.

Table S5. Comparison of the activity of FeNC800 with previous reports

Catalyst	Catalyst (mg)	Substrate (mmol)	Hydrazine (mmol)	T (°C)	Time	Yield (%)	Ref.
Co@NC	10	1	0.4mL	80	30min	97	[3]
Co@NCT-800	5	0.25	1mL	40	20min	99	[4]
Zn-N-C-1223	10	1	4	60	2.7h	99	[5]
Co-Mo$_2$C/AC	94	1	2 equiv.	80	2h	100	[6]
Ni$_2$P-AC	30	1	0.5mL	70	2h	93	[7]
CuNCNT	5	1	3	80	1h	99	[8]
In-situ Fe$_3$O$_4$	0.25 mol%	2	3.6	150	2min	99	[9]
Fe/Fe$_3$C@NC750	20	1	4	60	1h	100	[10]
Ni-WC	10	0.5	0.4mL	60	30min	99	[11]
Ni/SiO$_2$	10	6	48	100	8h	97.8	[12]
MnO$_2$	0.15mmol	0.5	1.5	25	6h	99	[13]

MoOxNy-550 (2 : 1)	20	0.5	0.75	30	50min	99	[14]
CuO	80	0.3mL	0.6mL	rt.	45s	98	[15]
FeSA@NC-20A	10	1	3	rt	30min	99	[16]
$Zr_{0.025}Fe_{0.975}Oy$-350	30	1	3	rt	4h	100	[17]
$Ce_{0.025}$-Fe_2O_3-350 °C	30	1	1.5	rt	10h	99	[18]
FeNC800	10	1	4	30	2h	98	this work

References

[1] M. Cheng, R. Ma, G. Chai, Y. Chen, L. Bai, D. Wang, J. Qian and G. H. Chen, Chem. Eng. J., 2023, 453, 139810.

[2] S. Wu, X. Pan, S. Xu, Y. Lin, H. Yan, G. Wen, J. Diao and H. Liu, Chem. Commun., 2020, 56, 3789–3792.

[3] S. Chen, L. Ling, S. Jiang and H. Jiang, Green Chem., 2020, 22, 5730-5741.

[4] Z. Zhang, Y. Liu, J. Du, Y. Jiang, Z. Wang, R. Yun and B. Zheng, Inorg. Chem. Front., 2023, 10, 7028-7037.

[5] Y. Song, R. Guo, B. Feng, Y. Fu, F. Zhang, Y. Zhang, D. Chen, J. Zhang and W. Zhu, Chem. Eng. J., 2023, 465, 142920.

[6] Z. Zhao, H. Yang, Y. Li and X. Guo, Green Chem., 2014, 16, 1274-1281.

[7] D. Sharma, P. Choudhary, S. Kumar and V. Krishnan, J. Colloid Interf. Sci., 2024, 657, 449-462.

[8] S. Wu, M. Zhao, Z. Xia, J. Liu, Y. Chen and Z. Xie, Mol. Catal., 2023, 550, 113583.

[9] D. Cantillo, M. Baghbanzadeh and C. O. Kappe, Angew. Chem. Int. Ed., 2012, 51, 10190-10193.

[10] B. Feng, Q. Xu, X. Wu, C. Ye, Y. Fu, D. Chen, F. Zhang and W. Zhu, Appl. Surf. Sci., 2021, 557, 149837.

[11] Y. Ma, Z. Lang, J. Du, L. Yan, Y. Wang, H. Tan, S.U. Khan, Y. Liu, Z. Kang and Y. Li, J. Catal., 2019, 377, 174-182.

[12] C. Jiang, Z. Shang and X. Liang, ACS Catal., 2015, 5, 4814-4818.

[13] C. Zhang, J. Lu, M. Li, Y. Wang, Z. Zhang, H. Chen and F. Wang, Green Chem., 2016, 18, 2435-2442.

[14] S. Luo, Y. Long, K. Liang, J. Qin, Y. Qiao, J. Li, G. Yang and J. Ma, Green Chem., 2021, 23, 8545-8553.

[15] K. Rajendran, N. Pandurangan, C.P. Vinod, T. Khan, S. Gupta, M. Haider and D. Jagadeesan, Appl. Catal. B: Environ., 2021, 297, 120417.

[16] G. Lu, K. Sun, Y. Lin, Q. Du, J. Zhang, K. Wang and P. Wang, Nano Res., 2022, 15, 603-611.

[17] T. Wan, G. Wang, Y. Guo, X. Fan, J. Zhao, X. Zhang, J. Qin, J. Fang, J. Ma and Y. Long, J. Catal., 2022, 414, 245-256.

[18] J. Zhao, G. Wang, Y. Gao, T. Wan, J. Qin, X. Zhang, F. Sun, J. Fang, J. Ma and Y. Long, ACS Sustainable Chem. Eng., 2023, 11, 5195-5205.